Supplementary Information: Breaking inversion symmetry by protonation: experimental and theoretical NEXAFS study of the diazynium ion, N_2H^+

Rafael C. Couto,[1] Weijie Hua,[2] Rebecka Lindblad,[3,4,5] Ludvig Kjellsson,[6,7] Stacey L. Sorensen,[3] Markus Kubin,[4] Christine Bülow,[4,8] Martin Timm,[4] Vicente Zamudio-Bayer,[4] Bernd von Issendorff,[8] Johan Söderström,[6] J. Tobias Lau,[4,8] Jan-Erik Rubensson,[6] Hans Ågren,[6,9] and Vincenzo Carravetta[10]

[1]*Department of Theoretical Chemistry and Biology, School of Chemistry, Biotechnology and Health, Royal Institute of Technology, SE-106 91 Stockholm, Sweden*
[2]*MIIT Key Laboratory of Semiconductor Microstructure and Quantum Sensing, Department of Applied Physics, School of Science, Nanjing University of Science and Technology, Nanjing 210094, China*
[3]*Department of Physics, Lund University, Box 118, S-22100 Lund, Sweden*
[4]*Abteilung für Hochempfindliche Röntgenspektroskopie, Helmholtz-Zentrum Berlin für Materialien und Energie, Albert-Einstein-Str. 15, 12489 Berlin, Germany*
[5]*Inorganic Chemistry, Department of Chemistry - Ångström Laboratory, Uppsala University , SE-75121 Uppsala , Sweden*
[6]*Department of Physics and Astronomy, Uppsala University, Box 516, SE-751 20 Uppsala, Sweden*
[7]*European XFEL GmbH, Holzkoppel 4, 22869 Schenefeld, Germany*
[8]*Physikalisches Institut, Albert-Ludwigs-Universität Freiburg, Hermann-Herder-Str. 3, 79104 Freiburg, Germany*
[9]*Tomsk State University, 36 Lenin Avenue, Tomsk, Russia*
[10]*IPCF-CNR, via Moruzzi 1, 56124 Pisa, Italy*

(Dated: July 26, 2021)

I. Computational details of vibrational analysis

Vibrationally-resolved N1s XAS for the π^*_{xz} states of N_2 and N_2H^+ were performed using a modified version of the DynaVib package[1] interfaced to GAMESS-US[2, 3] for electronic structure calculations. The density functional theory (DFT) method with the BLYP[4] functional was employed. A double-basis set technique[5] was also adopted. Basis sets for the ground and excited core hole (XCH) states are provided in Table S2. The protocol was recently verified to produce accurate vibrationally-resolved X-ray photoelectron spectra (XPS) at the C1s edge for a series of cyclic molecules.[5] For N_2, the computation of XAS is straightforward. Geometry optimizations were respectively performed for the ground and the XCH states, respectively. A fine integration grid and a tight gradient convergence tolerance (1×10^{-7} Hartree/Bohr) was employed. The vibrational frequencies were simulated at the ground state (GS) and the N1s XCH states, and then the Frank-Condon factors (FCFs) were simulated by using the Duschinsky rotation (DR)[6] method.

N_2H^+ has two non-equivalent nitrogens. We used a localized core hole picture and calculated the two nitrogens separately. Thus, for clarity, in the following equations we omit the explicit dependence on N_a and N_b. The ground state geometry of N_2H^+ is linear. While for either N1s XCH state, our calculations show that there is no linear minimum. Only a linear saddle point (minima along the stretching modes, maxima along the degenerate bending modes) exists. We first computed the FCFs of three modes (two stretching modes and the yz bending mode; see Figure S4) using the routine DR method. We found that only the two stretching modes are active. The yz bending mode is inactive since the potential energy surface (PES) of the π^*_{xz} core-excited state is similar to the ground-state PES except for a vertical shift.[7] Thus, we simply use $\Omega^{\text{strs}}_{lm}$ to denote the FC factors obtained from the DR method (l and m are quantum numbers for the N-N and N-H stretching modes, respectively.

To consider the effect of the xz bending mode, we computed the PESs for both XCH states along this mode. It was found that the core excited PESs have a double-well shape (Figure S2). The one dimensional nuclear Schrödinger equation

$$-\frac{1}{2}\frac{\partial^2}{\partial Q_j^2}|\psi_{jn}\rangle + V_j(Q_j)|\psi_{jn}\rangle = E_{jn}|\psi_{jn}\rangle, \tag{1}$$

was solved numerically by our in-house code. Here j is an index for the electronic state ($j = g, e$ for the ground and XCH state, respectively), $V_j(Q_j)$ represents the potential energy (atomic units used), n represents the quantum number for the bending vibration and Q_j stands for the normal coordinate of the xz bending mode. For each electronic state, we have chosen to expand respectively along its own normal coordinate. This is to get the best consistency with the DR calculations of the two stretching modes. Within this way, it is also straightforward to define the total vibrational energies while combing with the stretching modes (since each modes always have the same electronic reference). The Franck-Condon factor of this mode was then computed via

$$\Omega^{\text{bend}}_n = \langle\psi_{g0}(Q_g)|\psi_{en}(Q_e)\rangle^2 \approx \langle\psi_{g0}(Q)|\psi_{en}(Q)\rangle^2 \tag{2}$$

In practice, eq 2 was solved numerically by assuming the same normal coordinate Q. This approximation is reasonable considering the similarity of their normal coordinates, and the final spectra are numerically less sensitive to the computed FC factors of this bending mode. The total FC factors are given by

$$\Omega^{\mathrm{tot}}_{nlm} = \Omega^{\mathrm{bend}}_{n}\Omega^{\mathrm{strs}}_{lm}. \tag{3}$$

In practice, the above equations for N_a and N_b were solved independently in terms of relative vibrational energies (i.e. by setting 0-0 transition energies at 0). The N_a and N_b results were aligned to the computed adiabatic transition energies of N_a and N_b, and N_a and N_b contributions were weighted by their electronic oscillator strengths. Finally, stick spectra were convoluted and uniformly shifted to better compare with experiment.

Considering that the bending mode is described by a large displacement of the proton and much smaller variations of the N-N and N-H bond lengths, let us consider, in first approximation, the bending vibration in the ground state as the motion (in the x, y plane) of the proton in presence of a rigid N_2 fragment (oriented along the z axis) and fixed N-H bond length. Such decoupling is also justified by the difference in the vibrational frequencies. The proton motion can be described by the product of two degenerates wave functions Ψ_{b_x}, Ψ_{b_y} and then $\propto e^{-\omega(x^2+y^2)}$. However, moving to polar coordinates (ρ, ϕ) that better represents the cylindrically symmetry of the bending potential, we can easily see that the total wavefuntion is $\propto e^{-\omega\rho^2}$ i.e. a function of ρ only, as it is the potential, and the azimuthal dependence is only present in a complex phase factor $e^{-ik\phi}$. This wavefunction can then be seen as representing a bending vibration in the molecular plane and a free rotation around the z axis. By these considerations the calculation of the FC factors can be reduced, by the usual approximations, to the calculation of the overlap between stretching wave functions and a single bending wavefunction of initial and final electronic states.

Table S1. Analysis of the N_2H^+ RASPT2 results dependency of the size of active space (AC) and basis set (BS). It is shown the splitting between N_1 and N_2 π^* peaks ($N_b - N_a$) and the intensity ratio of them (in parenthesis - N_a/N_b). The active space column shows the number of orbitals, in RAS2, per irreducible representation in the C_{2v} symmetry (a_1, b_1, b_2 and a_2, respectively). The basis set considered is the aug-cc-pVXZ (X = D, T, Q, 5).

AC / BS	ACDZ	ACTZ	ACQZ	AC5Z
4 2 2 0	0.39 (2.01)	0.57 (2.02)	0.59 (1.99)	0.59 (1.92)
5 2 2 0	0.44 (1.98)	0.58 (2.06)	0.57 (2.05)	0.55 (1.96)
6 2 2 0	0.22 (2.32)	0.28 (2.31)	0.30 (2.19)	0.29 (2.04)
4 3 3 0	0.33 (1.81)	0.47 (2.01)	0.54 (1.82)	0.53 (1.74)
5 3 3 0	0.39 (2.05)	0.35 (2.42)	0.32 (2.48)	0.28 (2.27)
6 3 3 0	0.18 (2.66)	0.29 (1.92)	0.32 (1.81)	0.32 (1.72)
4 4 4 0	0.39 (1.85)	0.46 (1.77)	0.46 (1.72)	0.44 (1.62)
5 4 4 0	0.37 (1.99)	0.37 (2.02)	0.35 (1.97)	0.32 (1.83)
6 4 4 0	0.15 (2.45)	0.10 (3.12)	0.11 (2.59)	0.08 (2.26)
4 2 2 1	0.37 (2.01)	0.55 (2.01)	0.57 (1.97)	0.58 (1.91)
5 2 2 1	0.42 (1.98)	0.56 (2.05)	0.56 (2.04)	0.54 (1.95)
6 2 2 1	0.20 (2.38)	0.27 (2.32)	0.29 (2.20)	0.28 (2.04)
4 3 3 1	0.31 (1.87)	0.47 (1.80)	0.50 (1.76)	0.51 (1.70)
5 3 3 1	0.37 (2.05)	0.34 (2.41)	0.30 (2.48)	0.27 (2.26)
6 3 3 1	0.18 (2.73)	0.28 (1.92)	0.32 (1.81)	0.32 (1.72)
4 4 4 1	0.37 (1.89)	0.45 (1.82)	0.45 (1.79)	0.42 (1.67)
5 4 4 1	0.36 (2.03)	0.36 (2.10)	0.34 (2.07)	0.31 (1.92)
6 4 4 1	0.15 (2.55)	0.09 (3.44)	0.11 (2.77)	0.07 (2.46)
4 2 2 2	0.36 (2.01)	0.55 (2.00)	0.56 (1.97)	0.57 (1.90)
5 2 2 2	0.42 (1.98)	0.56 (2.05)	0.55 (2.03)	0.54 (1.94)
6 2 2 2	0.20 (2.41)	0.26 (2.34)	0.29 (2.19)	0.27 (2.05)
4 3 3 2	0.31 (1.91)	0.49 (1.81)	0.52 (1.77)	0.54 (1.71)
5 3 3 2	0.37 (2.06)	0.34 (2.42)	0.31 (2.48)	0.27 (2.28)
6 3 3 2	0.17 (2.78)	0.28 (1.94)	0.32 (1.83)	0.32 (1.73)
4 4 4 2	0.38 (1.90)	0.45 (1.85)	0.44 (1.82)	0.42 (1.71)
5 4 4 2	0.36 (2.04)	0.36 (2.15)	- (-)	0.32 (1.98)
6 4 4 2	0.14 (2.61)	0.10 (3.42)	0.11 (2.77)	0.08 (2.45)

Table S2. Basis sets used for DFT calculations of ground (GS) and core excited (XCH) states of N_2H^+; the asterisk marks the atom with the excited core.

Basis set	χ_{GS}	χ_{XCH}
N*	cc-pVTZ[8, 9]	IGLO-III [10]
N	cc-pVTZ	MCP-TZP[11–13]
H	cc-pVTZ	cc-pVTZ

Table S3. Atom-specific (N_a, N_b) energies and their differences (N_b-N_a) of N_2H^+ predicted by different methods (all in eV): Vertical and adiabatic transition energies (E_1^{vert}, E_1^{ad}) to the first N 1s core-excited state e (1s$\rightarrow\pi^*$), and vertical ionic potential (IP^{vert}). Note the order switch of E_1^{vert} and E_1^{ad} difference (bolded faces). No *ad hoc* shift was applied in this table. The RASPT2 results were obtained with the aug-cc-pVTZ basis set, active space of 8 electrons in 7 orbitals and no symmetry constrains were considered.

Method	atom	E_1^{ad}	ΔZPE	E_1^{vert}	f_1	IP^{vert}
BLYP	N_a	400.430	-0.057	400.531	0.038	420.719
	N_b	400.383	-0.084	400.887	0.027	420.499
	N_b-N_a	**-0.043**	-0.027	**0.357**	–	-0.220
B3LYP	N_a	401.275	-0.064	401.379	0.038	420.893
	N_b	401.200	-0.093	401.717	0.026	420.648
	N_b-N_a	**-0.076**	-0.029	**0.338**	–	-0.245
CAM-B3LYP	N_a	402.231	-0.070	402.330	0.038	421.010
	N_b	402.156	-0.099	402.671	0.026	420.765
	N_b-N_a	**-0.075**	-0.029	**0.342**	–	-0.246
M06-2X	N_a	402.790	-0.060	402.844	0.035	421.056
	N_b	402.545	-0.095	403.000	0.026	420.613
	N_b-N_a	**-0.245**	-0.035	**0.156**	–	-0.443
RASPT2	N_a	402.988		403.320	0.051	421.992
	N_b	402.896		403.566	0.063	422.319
	N_b-N_a	**-0.093**		**0.246**	–	0.328

[a] ΔZPE: the ZPE difference of e relative to the ground state.
[b] f_1: the electronic oscillator strength (arb. unit) for vertical excitation to e.

Table S4. Computed FCFs for the two stretching modes (modes 3, 4) of N_2H^+ for the 1s→LUMO excitations of N_a and N_b. Only transitions with the FC factor $\Omega^{strs} > 0.1$ are listed.

N_a			N_b		
E(eV)	Ω^{strs}	transition	E(eV)	Ω^{strs}	transition
0.000	0.6541	$0\rightarrow 0$	0.000	0.1249	$0\rightarrow 0$
0.252	0.2536	$0\rightarrow 1_3$	0.213	0.2743	$0\rightarrow 1_3$
0.503	0.0359	$0\rightarrow 2_3$	0.426	0.2634	$0\rightarrow 2_3$
			0.639	0.1430	$0\rightarrow 3_3$
			0.852	0.0470	$0\rightarrow 4_3$
			0.420	0.0165	$0\rightarrow 1_4$
			0.633	0.0326	$0\rightarrow 1_3 1_4$
			0.846	0.0275	$0\rightarrow 2_3 1_4$
			1.059	0.0127	$0\rightarrow 3_3 1_4$

Table S5. Computed FCFs for the bending mode (1D model) of N_2H^+ for the 1s→LUMO excitations of N_a and N_b. Only levels of eigenstates with even parity (corresponding to even n)[a] have nonzero FCFs.

n	N_a		N_b	
	E(eV)	Ω^{bend}	E(eV)	Ω^{bend}
0	0.000	0.009	0.000	0.193
2	0.124	0.054	0.098	0.598
4	0.234	0.196	0.192	0.188
6	0.325	0.419	0.321	0.019
8	0.404	0.252	0.464	0.002
10	0.497	0.056		
12	0.597	0.011		
14	0.696	0.002		
16	0.791	0.001		

[a] n denotes the vibrational quantum number of mode 2 (the bending mode) the core-excited state.

Table S6. Interpretation of major vibrational transitions (a threshold of $\Omega^{\text{tot}} > 0.03$ was used; in descending order) for the N 1s → LUMO transitions of N_2H^+ (see Figure 7 in the text).[a,b]

E(eV)	Ω^{tot}	n	l	m	transition
N_a					
399.990	0.006	0	0	0	$0 \rightarrow 0$
0.325	0.274	3	0	0	$0 \rightarrow 3_2$
0.405	0.165	4	0	0	$0 \rightarrow 4_2$
0.234	0.128	2	0	0	$0 \rightarrow 2_2$
0.577	0.106	3	1	0	$0 \rightarrow 3_2 1_3$
0.656	0.064	4	1	0	$0 \rightarrow 4_2 1_3$
0.486	0.050	2	1	0	$0 \rightarrow 2_2 1_3$
0.497	0.036	5	0	0	$0 \rightarrow 5_2$
0.124	0.036	1	0	0	$0 \rightarrow 1_2$
N_b					
400.178	0.024	0	0	0	$0 \rightarrow 0$
0.311	0.164	1	0	0	$0 \rightarrow 1_2$
0.524	0.157	1	2	0	$0 \rightarrow 1_2 2_3$
0.737	0.085	1	3	0	$0 \rightarrow 1_2 3_3$
0.098	0.075	1	0	0	$0 \rightarrow 1_2$
0.213	0.053	0	1	0	$0 \rightarrow 0_2 1_3$
0.405	0.052	2	1	0	$0 \rightarrow 2_2 1_3$
0.426	0.051	0	2	0	$0 \rightarrow 0_2 2_3$
0.618	0.050	2	2	0	$0 \rightarrow 2_2 2_3$

[a] n, l, m denote the vibrational quantum numbers of modes 2 (bending), 3 (N-N stretching), 4 (N-H stretching) of the core-excited state.

[b] The 0-0 transition was also printed as a reference with absolute transition energies given. For the rest, relative energies were used.

Table S7. Cartesian coordinates (in Å) of BLYP-optimized stationary structures. For each nitrogen (N_a or N_b), the lowest N1s core-excited state structure was optimized in the vicinity of the ground state which has linear structure. No minimum with linear structure was found for the core-excited state; saddle point was found instead.

	Minimum, Ground state		
N_a	0.0000000000	0.0000000000	-0.5542580446
N_b	0.0000000000	0.0000000000	0.5445989053
H	0.0000000000	0.0000000000	1.5886591393
	Saddle, N_a 1s→LUMO		
N_a	0.0000000000	0.0000000000	-0.5824718227
N_b	0.0000000000	0.0000000000	0.5562499544
H	0.0000000000	0.0000000000	1.6052218683
	Saddle, N_b 1s→LUMO		
N_a	0.0000000000	0.0000000000	-0.6086874862
N_b	0.0000000000	0.0000000000	0.5880977561
H	0.0000000000	0.0000000000	1.5995897300

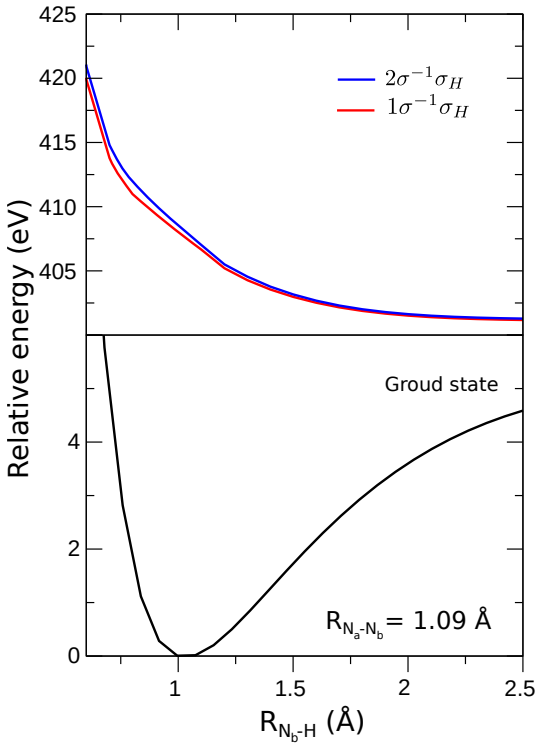

Figure S1. N_2H^+ RASPT2 potential energy curve of ground state (bottom) and $1s\sigma^*$ (top) for N_a (2σ) and N_b (1σ), illustrating the the strong dissociative character of the $1s\sigma^*$ excitation. The N_a-N_b distance was fixed at 1.09 Å, which corresponds to the equilibrium bond lenght.

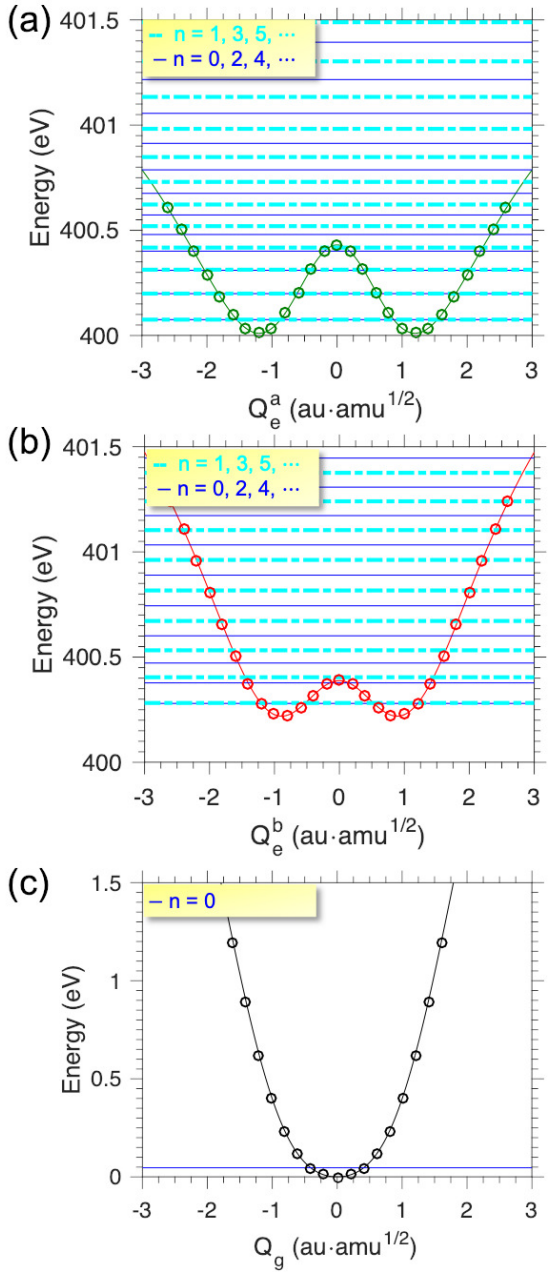

Figure S2. PESs of N_2H^+ for (a) N_a 1s→LUMO state (π_{xz}^*); (b) N_b 1s→LUMO state (π_{xz}^*); and (c) the ground state along the xz bending mode (mode 2). PES of each electronic state was computed by BLYP[14] (circles) along its own bending normal coordinate, and fitted by splines (curves). Low-lying vibrational levels were shown as horizontal lines (blue solid, $n = 0, 2, 4, \cdots$; cyan dashed, $n = 1, 3, 5, \cdots$).

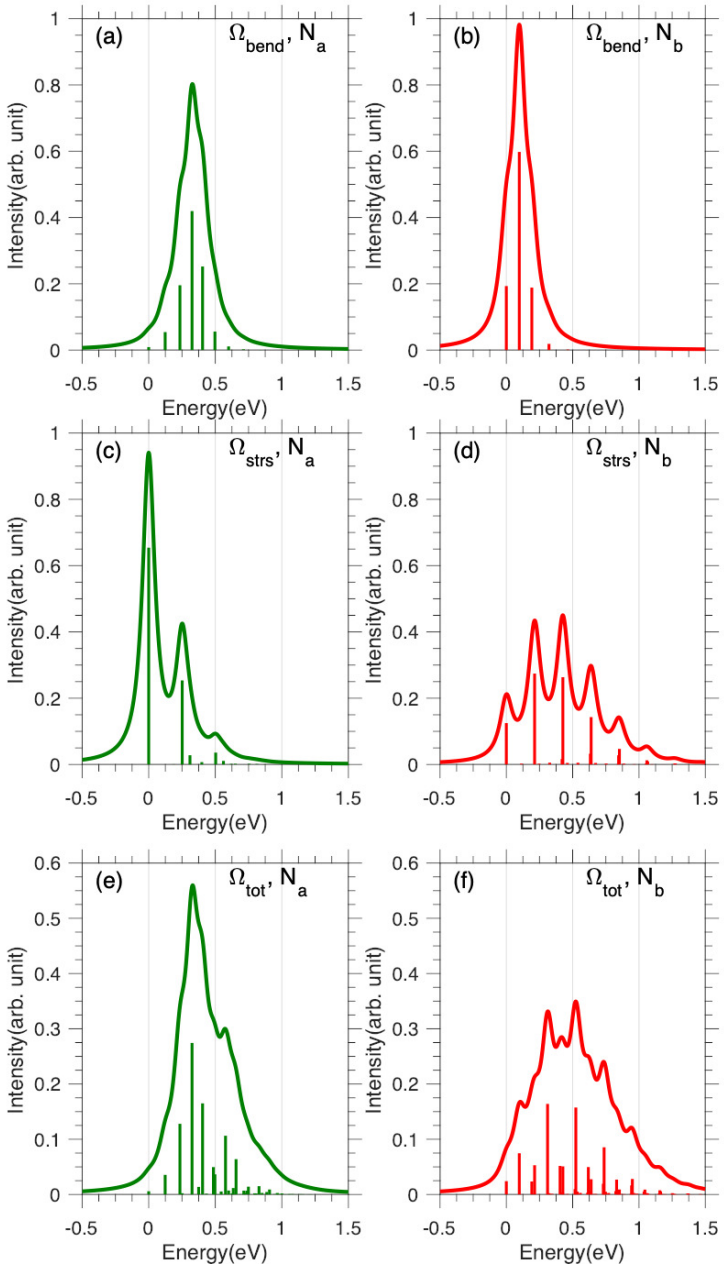

Figure S3. Computed FCFs of N_2H^+ combining the bending mode and the two stretching modes for the N1s→LUMO excitation: FCFs for the (a-b) bending mode, (c-d) stretching modes, and (e-f) combined results. Lorentzian line shape with HWHM of Γ_L=0.0565 eV was employed and relative energies were used. The absolute 0-0 transition energies in the total spectra are 400.0 and 400.2 eV for N_a and N_b, respectively.

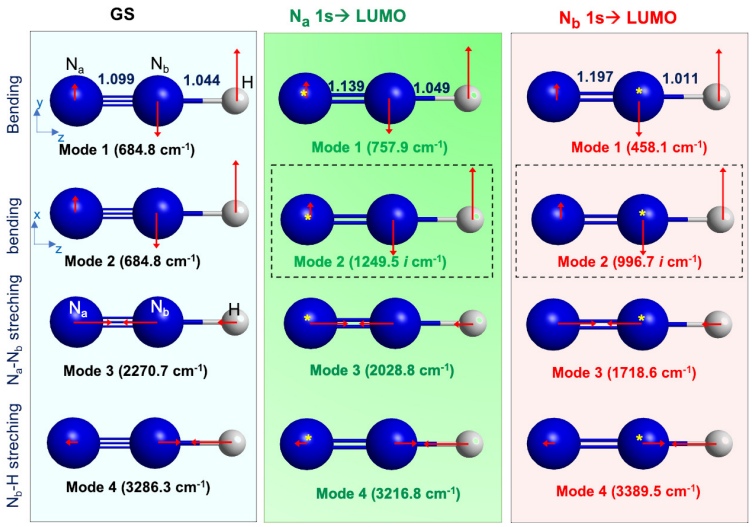

Figure S4. Computed vibrational modes of N_2H^+ by BLYP at the optimized (a) ground (b) XCH_a and (c) XCH_b state geometries. In panels b and c, dashed box strengthens the bending mode (mode 2)[15] with imaginary frequency, and star denotes the N1s core hole. All structures are linear with bond lengths labeled in Å.

[1] G. Tian, S. Duan, W. Hua and Y. Luo, *DynaVib, version 1.0*, Royal Institute of Technology: Sweden, 2012.
[2] M. W. Schmidt, K. K. Baldridge, J. A. Boatz, S. T. Elbert, M. S. Gordon, J. H. Jensen, S. Koseki, N. Matsunaga, K. A. Nguyen, S. Su, T. L. Windus, M. Dupuis and J. A. Montgomery Jr, *J. Comput. Chem.*, 1993, **14**, 1347–1363.
[3] M. S. Gordon and M. W. Schmidt, in *Advances in electronic structure theory: GAMESS a decade later*, ed. C. E. Dykstra, G. Frenking, K. S. Kim and G. E. Scuseria, Elsevier, Amsterdam, 2005, ch. 41, pp. 1167–1189.
[4] A. D. Becke, *Phys. Rev. A*, 1988, **38**, 3098.
[5] W. Hua, G. Tian and Y. Luo, *Phys. Chem. Chem. Phys.*, 2020, **22**, 20014–20026.
[6] F. Duschinsky, *Acta Physicochim. URSS*, 1937, **7**, 551–566.
[7] J.-i. Adachi, N. Kosugi and A. Yagishita, *J. Phys. B: At. Mol. Opt. Phys.*, 2005, **38**, R127–R152.
[8] T. H. Dunning, *J. Chem. Phys.*, 1989, **90**, 1007–1023.
[9] R. A. Kendall, T. H. Dunning and R. J. Harrison, *J. Chem. Phys.*, 1992, **96**, 6796–6806.
[10] W. Kutzelnigg, U. Fleischer and M. Schindler, *Deuterium and shift calculation*, Springer, 1990, pp. 165–262.
[11] Y. Sakai, E. Miyoshi, M. Klobukowski and S. Huzinaga, *J. Chem. Phys.*, 1997, **106**, 8084–8092.
[12] T. Noro, M. Sekiya and T. Koga, *Theor. Chem. Acc.*, 1997, **98**, 25–32.
[13] E. Miyoshi, H. Mori, R. Hirayama, Y. Osanai, T. Noro, H. Honda and M. Klobukowski, *J. Chem. Phys.*, 2005, **122**, 074104.
[14] In this work, the BLYP total energy and vibrational frequencies at each optimized geometry were generated with C_{4v} symmetry (recommened by GAMESS-US for linear molecules). While for PES generation along the bending mode, the C_1 symmetry was set. Tests show that C_1 symmetry at the same geometry (optimized structures for the two XCH states) gives total energy that is 0.01 a.u. higher than C_{4v}. To remove the influence of this inconsistency, we uniformly shifted the core-state PESs by calibrating to the C_{4v} results. Since the shifts are almost the same for N_a and N_b, we verify that this technical issue does not affect our conclusions.
[15] The orders of vibrational modes from the raw GAMESS-US output have been adjusted to match those of the ground state.